

ORIGINAL RESEARCH

Disrupted Blood-Brain Barrier and Mitochondrial Impairment by Autotaxin–Lysophosphatidic Acid Axis in Postischemic Stroke

Susmita Bhattarai , MS; Sudha Sharma, MS; Hosne Ara, MD, PhD; Utsab Subedi, MS, MPH; Grace Sun ; Chun Li, MD, PhD; Md. Shenuarin Bhuiyan , PhD; Christopher Kevil , PhD; William P. Armstrong, MS; Miles T. Minvielle , MS; Sumitra Miriyala, PhD; Manikandan Panchatcharam , PhD

BACKGROUND: The loss of endothelial integrity increases the risk of intracerebral hemorrhage during ischemic stroke. Adjunct therapeutic targets for reperfusion in ischemic stroke are in need to prevent blood-brain barrier disruption. Recently, we have shown that endothelial permeability is mediated by lysophosphatidic acid (LPA), but the role of autotaxin, which produces LPA, remains unclear in stroke. We investigate whether autotaxin/LPA axis regulates blood-brain barrier integrity after cerebral ischemia.

METHODS AND RESULTS: Ischemic stroke was induced in mice by middle cerebral artery occlusion for 90 minutes, followed by 24-hour reperfusion. The therapeutic efficacy of autotaxin/LPA receptor blockade was evaluated using triphenyl tetrazolium chloride staining, Evans blue permeability, infrared imaging, mass spectrometry, and XF24 analyzer to evaluate blood-brain barrier integrity, autotaxin activity, and mitochondrial bioenergetics. In our mouse model of ischemic stroke, the mRNA levels of autotaxin were elevated 1.7-fold following the cerebral ischemia and reperfusion (I/R) group compared with the sham. The enzymatic activity of autotaxin was augmented by 4-fold in the I/R group compared with the sham. Plasma and brain tissues in I/R group showed elevated LPA levels. The I/R group also demonstrated mitochondrial dysfunction, as evidenced by decreased ($P < 0.01$) basal oxygen consumption rate, mitochondrial ATP production, and spare respiratory capacity. Treatment with autotaxin inhibitors (HA130 or PF8380) or autotaxin/LPA receptor inhibitor (BrP-LPA) rescued endothelial permeability and mitochondrial dysfunction in I/R group.

CONCLUSIONS: Autotaxin-LPA signaling blockade attenuates blood-brain barrier disruption and mitochondrial function following I/R, suggesting targeting this axis could be a new therapeutic approach toward treating ischemic stroke.

Key Words: autotaxin ■ blood-brain barrier ■ ischemic stroke ■ lysophosphatidic acid ■ permeability ■ superoxide radicals

Ischemic stroke, a vascular blockage in the brain, is a leading cause of death in the United States, responsible for 1 of every 20 deaths. Stroke results in varying levels of disability among recovered patients; the cost of poststroke care, which can be prohibitive, is one of the most expensive consequences of stroke. The United States spends the most on poststroke care, causing

an economic burden on families and society.¹ Despite the major limitation of a short therapeutic window of ≈4.5 hours, recombinant tPA (tissue-type plasminogen activator) is the only therapy available for use in treating acute ischemic stroke. Several other treatments tested for stroke have not been introduced for use because they lacked effectiveness. Although recombinant tPA is

Correspondence to: Sumitra Miriyala, PhD, and Manikandan Panchatcharam, PhD, Department of Cellular Biology and Anatomy, Louisiana State University Health Sciences Center–Shreveport, PO Box 33932, Shreveport, LA 71130-3932. E-mail: smiriy@lsuhsc.edu and mpanch@lsuhsc.edu

Supplementary Material for this article is available at <https://www.ahajournals.org/doi/suppl/10.1161/JAHA.121.021511>

For Sources of Funding and Disclosures, see page 12.

© 2021 The Authors. Published on behalf of the American Heart Association, Inc., by Wiley. This is an open access article under the terms of the Creative Commons Attribution-NonCommercial License, which permits use, distribution and reproduction in any medium, provided the original work is properly cited and is not used for commercial purposes.

JAHA is available at: www.ahajournals.org/journal/jaha

CLINICAL PERSPECTIVE

What Is New?

- Autotaxin–lysophosphatidic acid (LPA) axis could play a critical role in pathophysiological effects during ischemic stroke.
- Herein, we show that LPA is increased along with autotaxin following ischemic stroke.
- We evaluate the effect of the autotaxin-LPA axis in elevated permeability following ischemic stroke.
- Autotaxin-LPA axis affects the mitochondrial bioenergetics in the brain after ischemic stroke.

What Are the Clinical Implications?

- Autotaxin inhibitors could be implemented to manage ischemic stroke as the autotaxin-LPA axis increases endothelial permeability in our in vivo stroke model.
- We elucidate the effect caused by elevated LPA following ischemic stroke so that LPA could be considered a marker for stroke management.

Nonstandard Abbreviations and Acronyms

BBB	blood-brain barrier
I/R	ischemia and reperfusion
LPA	lysophosphatidic acid
MCAO	middle cerebral artery occlusion
OCR	oxygen consumption rate
SOD	superoxide dismutase
TTC	triphenyl tetrazolium chloride

in use, only 3% to 5% of patients with stroke are eligible to receive it, as most other patients with stroke are at risk for intracerebral hemorrhage.² Apart from recombinant tPA, mechanical thrombectomy is limited in use because of a lack of expertise and resources, and it is useful for only about 9% of patients with proximal large-artery occlusion.^{3–5} Better therapeutic strategies are necessary to improve the outcome for patients with ischemic stroke by lowering death rates and improving the quality of life of ischemic stroke survivors.

Microvascular endothelial cells, tight junctions, and adherens junctions help the brain maintain its security system (blood-brain barrier [BBB]), which ultimately protects the central nervous system. Astrocytes and microglial cells⁶ support the maintenance of the BBB. Breakdown of the BBB may initiate adverse clinical outcomes after ischemic strokes, such as elevated interendothelial permeability.⁷ Disruption in BBB following an ischemic stroke leads to edema, hemorrhage,

and the infiltration of immune cells in the brain, resulting in clinical deterioration.⁸ BBB disruption⁷ aids pathological progression of ischemic stroke. Junctional proteins, such as zonula occludens-1, claudin-5, vascular endothelial cadherin, and β -catenin, are essential for BBB maintenance, and their modulation could be used as a therapeutic target in ischemic stroke.⁶ The maintenance of dynamic regulation of junctional proteins protects the vasculature, resulting in reduced risk of hemorrhage and ultimately controlling the progression of the disease.⁹ So, targeting junctional proteins represents a new path for the treatment of ischemic stroke, which is also the main focus in this study.^{9,10}

Lysophosphatidic acid (LPA) is a phospholipid with a glycerol backbone, a hydroxyl group, phosphate, and a saturated or unsaturated fatty acid chain.¹¹ LPA is generated in the blood plasma of humans and rodents by hydrolysis of circulating lysophospholipids, which are catalyzed by the lysophospholipase D enzyme autotaxin when the concentration is >100 nmol/L.^{12,13} The several physiological effects of LPA occur through the actions of 6 LPA receptors and their genes, namely LPA receptor (LPAR) 1 to LPAR6 (human) and Lpar1 to Lpar6 (nonhuman).¹⁴ LPA has been detected in higher than normal concentrations in other diseases as well, such as vascular dementia, spinal cord injury, fibrosis, cardiovascular diseases, cancer, and Alzheimer disease.^{15,16} It has been suggested that LPA could serve as a biomarker for these diseases and could be a biomarker of stroke, as shown by our study.

The effect of LPA on endothelial cells has been shown to increase the phosphorylation of endothelial NO synthase on serine 1179, leading to endothelial NO synthase activation in aortic endothelial cells.¹⁷ Lysophosphatidylcholine and its product LPA activate nicotinamide adenine dinucleotide phosphate oxidase 2, leading to increased reactive oxygen species formation¹⁸ in pulmonary microvascular endothelial cells.¹⁹ These studies indicate that LPA and its downstream signaling disrupt the balance of the oxidative equilibrium in endothelial cells. Decreased mitochondrial membrane potential, along with reduced ATP levels, were also observed in coronary artery endothelial cells and cardiomyocytes treated with LPA.^{18,20} In particular, LPA has been shown to increase permeability in cultured brain microvascular endothelial cells.^{21–23} However, the extent of destruction caused by autotaxin/LPA in brain endothelial cells, leading to endothelial permeability and disruption of junctional proteins, has yet to be explored. In this study, the focus is to determine the role and effect of LPA and its regulator enzyme autotaxin in stroke.

METHODS

All data and supporting materials have been provided with the published article.

Animal Models of Ischemic Stroke

Animal handling and surgical procedures and protocols were approved by the Institutional Animal Care and Use Committee at Louisiana State University Health Science Center–Shreveport. They were performed in accordance with the National Institutes of Health *Guide for the Care and Use Laboratory Animals*. C57BL6/J male mice (3 months old) were used for the surgery. In the animals that underwent cerebral ischemia and reperfusion (I/R), ischemic stroke was induced by right middle cerebral artery occlusion (MCAO) for 90 minutes and reperfusion for 24 hours. Mice were anesthetized with isoflurane (induction at 5% and maintenance at 1.5%) in a gas mixture containing 30% O₂/70% N₂ via a facemask and kept on a temperature-controlled heating pad (Harvard Apparatus, March, Germany), which maintained the rectal temperature at 37 °C throughout the surgery. A laser-Doppler flow probe (PERIMED, PF 5010 LDPM Unit, Sweden) was attached to the right side of the dorsal surface of the skull to monitor regional cerebral blood flow. The right common and external carotid arteries were exposed and ligated. The middle cerebral artery was occluded by the insertion of a silicone rubber-coated monofilament (Doccol Corporation, MA); through the basal part of the external carotid artery, the monofilament was advanced cranially into the internal carotid artery to the point where the middle cerebral artery branches off from the internal artery. An immediate decrease in regional cerebral blood flow indicated the onset of MCAO. In the sham group, the monofilament was also inserted into the internal carotid artery but not to the point that it causes a reduction in regional cerebral blood flow. Reperfusion was induced at 90 minutes of MCAO by suture withdrawal and reopening the right common carotid artery. After the surgery, mice were given carprofen (2 mg/kg) postoperative by subcutaneous injection and placed in a heating pad. Animals were observed for at least 30 minutes to 1 hour to ensure that they show no surgery's ill effects. During this recovery period, any mice unable to right themselves (like spinning in place or paresis) were euthanized. To enable easy access to food, soft wet food is placed inside the cage. At 24 hours of reperfusion, the mice were euthanized by exposure to absolute isoflurane. Blood was collected, and the plasma was separated to measure the LPA concentration. Triphenyl tetrazolium chloride (TTC) staining was done in mouse brain tissues, cut in 1.5-mm sections. The infarct size in the corresponding areas was measured using Image J. Brain cortical tissues were collected for Western blotting analysis and reverse transcription–polymerase chain reaction.

In Vivo Imaging

Autotaxin activity in the mouse brain and brain slices was analyzed using a fluorogenic analog of

lysophosphatidylcholine (AR-2), enabling in vivo visualization of autotaxin activity. AR-2 activated by autotaxin exhibits fluorescence, and the fluorescence observed correlates directly with the activity of autotaxin. The assay was performed according to that used by Madan et al, with modifications.²⁴ AR-2, diluted in PBS, was injected intravenously via the lateral tail vein and administered at 0.5 mg/kg body weight 2 hours before brain collection. The fluorescence signal was acquired and analyzed using the LI-COR Odyssey (LI-COR Biosciences) in the brain sections. The autotaxin inhibitors PF8380 (30 mg/kg body weight) (Echelon Biosciences Inc, Logan, UT), HA130 (0.5 mg/kg body weight; 1 μL/g, 1 mmol/L) (Echelon Biosciences Inc), and BrP-LPA (10 mg/kg body weight) were injected intraperitoneally in mice 1 hour before MCAO surgery in the respective separate experimental groups.^{25–27} The effect of LPA on vascular permeability was examined, as shown previously.²⁶ Briefly, the mice were anesthetized and injected intravenously with Evans blue dye (0.1 mL of a 1% solution in PBS) at 6 hours of reperfusion. Fifteen minutes later, the anesthetized mice were perfused with PBS containing heparin through the right ventricle at a constant rate to yield pressure of 25 mm Hg. Evans blue dye, being a fluorophore,²⁸ is measured in 680 channels using the LI-COR Odyssey. The fluorescence intensity measured directly correlates to the amount of Evans blue dye permeabilized in the brain tissue.

Mitochondrial Bioenergetics

The oxygen consumption rate (OCR) was analyzed using a Seahorse extracellular flux analyzer (XF-24, Seahorse Biosciences, Chicopee, MA). The mitochondria was isolated from the peri-infarct I/R tissue and the corresponding areas of the sham mice. The mitochondrial bioenergetic measurements were performed according to the method described in Chandra et al,¹⁸ where different batches of mitochondria came from the same group. The real-time bioenergetic activity of mitochondria and the effects of treatments were observed as free protons, and the concentration of oxygen was measured using the XF-24. OCR was quantified in pmol/min per μg, with normalization, performed with respect to the total protein content. The initial basal value of OCR was interrupted by the addition of oligomycin (complex V inhibitor), giving values for ATP-linked OCR. Carbonyl cyanide p-trifluoromethoxyphenyl hydrazone (FCCP; an uncoupler) and rotenone+antimycin (complex I and complex III inhibitor) additionally determine maximal OCR capacity and spare OCR capacity, respectively.

Lysophosphatidylcholine and LPA Analysis Using Mass Spectrometry

For the quantification of lysophosphatidylcholine and LPA molecular species, we used high-performance

liquid chromatography–tandem mass spectrometry, as previously described.^{12,18,26} The abundance of the lysophosphatidylcholine/LPA in plasma was calculated as pmol/10 nmol PO₄²⁻ and finally normalized with the 18:1 lysophosphatidylcholine/LPA of the sham group, resulting in relative abundance.

Statistical Analysis

Data analysis was conducted using Graphpad Prism 8. Data are reported as mean±SD, with all experiments performed with a minimum of 3 replicates. One-way ANOVA, followed by the Tukey, post hoc test or the unpaired Mann-Whitney *U* test was used to identify significant differences between groups. A *P* value of <0.05 was considered significant. The study was randomized, and the investigators were blinded between the treatment groups.

An expanded Methods section is available in Data S1.

RESULTS

Elevated Autotaxin Activity Following I/R

The I/R was performed in 3-month-old male mice, and the 1.5-mm brain slices prepared were stained with TTC. TTC staining of the brains of mice who underwent I/R showed infarct regions in the right hemisphere of the brain, compared with slices from the sham mice (Figure 1A). The infarct area was measured with Image J and quantified as a percentage of the hemisphere. The brain cryosections showed microglial activation, indicating inflammation on the ipsilateral side of the I/R mouse brains, but not those of the sham mice (Figure 1B). The ipsilateral brains from I/R and sham mice were collected for reverse transcription–polymerase chain reaction, which showed that the level of autotaxin mRNA was significantly elevated in I/R mice to >1.7-fold higher than that of the sham mice (Figure 1C). As autotaxin is an enzyme, we were interested in assessing the activity following stroke. An AR-2 fluorescence assay was used to determine the activity of autotaxin *in vivo*. As shown in Figure 1D, the AR-2 fluorescence measured in I/R mice using the Li-COR Odyssey was significantly higher compared with that in the sham mice. The AR-2 fluorescence obtained correlates directly with the increased enzymatic activity of the autotaxin in the brain tissue in I/R mice. Saturated and unsaturated forms of lysophosphatidylcholine are the precursors for the different forms of LPA in circulation. Liquid chromatography–mass spectrometry analysis showed that there were no significant changes in lysophosphatidylcholine levels, except for the unsaturated 18:1 lysophosphatidylcholine, in the plasma of I/R compared with that of the sham mice (Figure 1E).

LPA Escalation Following I/R

As autotaxin was elevated following I/R, we then measured plasma LPA using liquid chromatography–mass spectrometry and found that 18:1, 16:0, 18:0, 20:4, and 22:6 were significantly elevated after I/R (Figure 2A). Following on from our observation of elevated LPA in plasma, we were interested in measuring LPA in brain tissue following I/R. We performed ELISA in the ipsilateral hemisphere brain tissue lysate, revealing a significant increase in LPA levels in I/R compared with sham (Figure 2B). Along with ELISA, immunofluorescence assays were performed in brain cryosections to detect LPA in brain tissue. Immunohistochemistry analysis (Figure 2C) revealed LPA in the ipsilateral area of I/R mouse brain tissue. There was a clear difference between the comparable regions of the brains of I/R mice compared with those of sham mice, with amplified LPA detection in the I/R tissue of both the infarct core and peri-infarct areas. With LPA detection in the I/R tissue, we observed an exciting finding of LPA being not present uniformly in the tissues but enhanced in a vascular distribution pattern. So immunofluorescence analysis of LPA and cluster of differentiation 31 (endothelial marker) was performed in these brain sections. We detected colocalization of enhanced LPA with cluster of differentiation 31 in I/R tissues (Figure 2D), suggesting LPA increase was confined to the brain microvessels following ischemic stroke. LPA was increased robustly in ipsilateral side compared with the contralateral side in I/R group (Figure 2D). Because LPA acts on cellular functions via its receptors, we performed reverse transcription–polymerase chain reaction for the receptors. Peri-infarct brain tissue yielded mRNA levels of all 6 known LPA receptors in the corresponding areas of the brain tissues. There was a significant increase in levels of LPAR1, LPAR2, LPAR5, and LPAR6, with LPAR5 having the highest (~5-fold) change in I/R mouse brains compared with those of sham mouse brains. LPAR3 was significantly reduced, whereas LPAR4 was not altered following I/R in mouse brains compared with levels in the sham brains (Figure 2E).

Autotaxin Inhibitors Decreased LPA Levels in MCAO Mice

Having observed elevated levels of autotaxin and LPA, we were interested in looking at the effects of autotaxin inhibitors on ischemic stroke. The autotaxin inhibitors PF8380 and HA130 were used in our MCAO mice model. PF8380 or HA130 was injected intraperitoneally 1 hour before MCAO surgery. Both inhibitors significantly reduced the activity of autotaxin compared with that in the sham group (Figure 3A). The relative abundance of lysophosphatidylcholine in plasma, measured with liquid chromatography–mass spectrometry in all experimental groups (sham, I/R, HA130

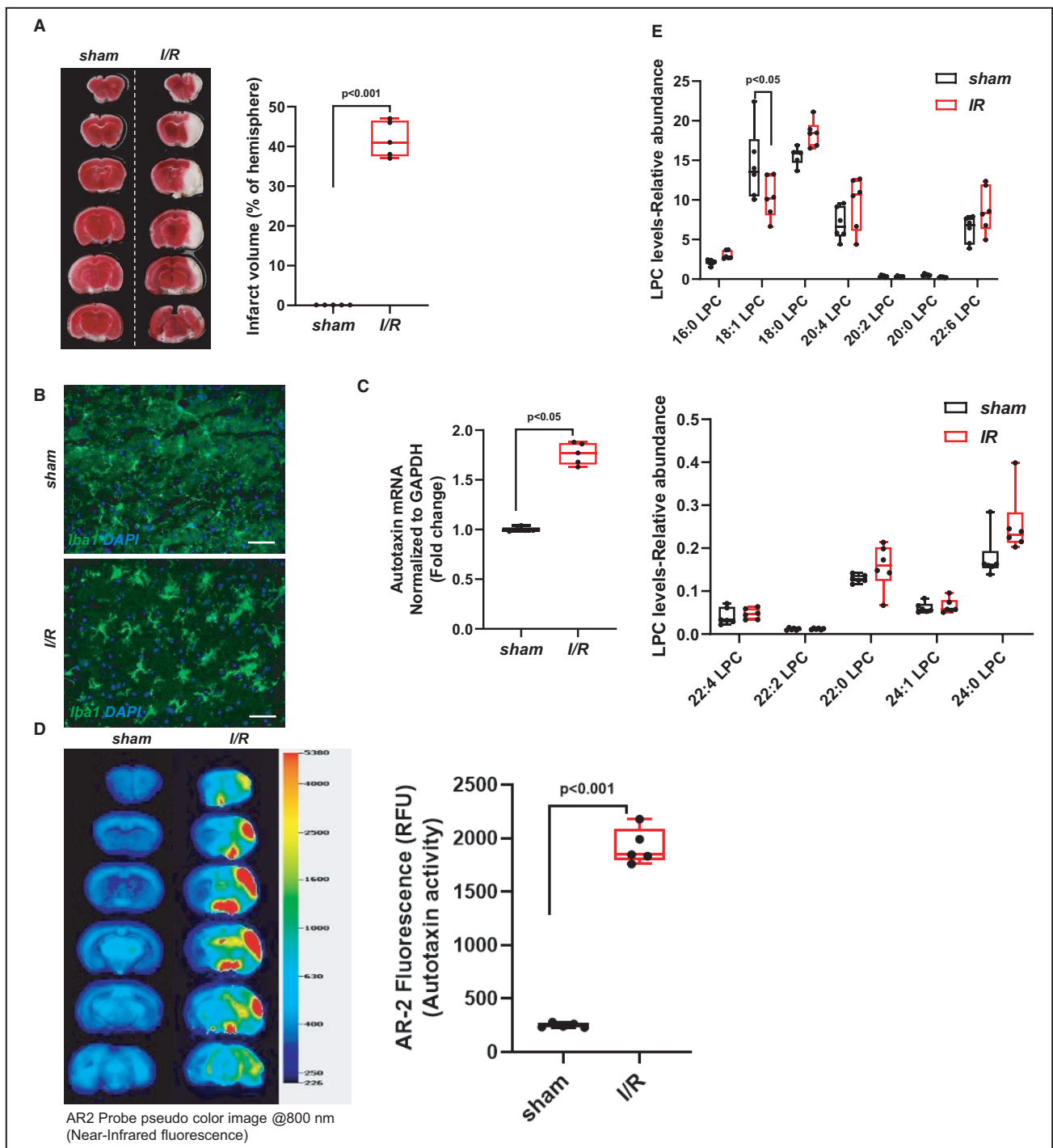


Figure 1. Elevated autotaxin (ATX) activity following ischemia and reperfusion (I/R).

A, Triphenyl tetrazolium chloride staining of mouse brain slices and respective infarct volume (percentage of the hemisphere) measured in sham and I/R mice. **B**, Mouse brain cryosections stained for microglia (Iba1) in sham and I/R mice ipsilateral cortex. Bar=200 μ m. **C**, ATX mRNA expression was measured in ipsilateral cortex brain tissue lysate from sham and I/R mice. **D**, Enzymatic activity test for ATX measured with AR-2 fluorescence, quantified as relative fluorescence unit (RFU) in sham and I/R mouse brain slices. **E**, Lysophosphatidylcholine subspecies in plasma from sham and I/R mice, measured with liquid chromatography–mass spectrometry, quantified relative to 18:1 LPC. All values are mean \pm SD compared with the sham group using Mann-Whitney *U* test. DAPI indicates 4',6-diamidino-2-phenylindole. NI, near-infrared.

treated, and PF8380 treated), showed no significant differences between the groups, except a decrease in 18:1 lysophosphatidylcholine in I/R mouse brains,

which was significantly reduced compared with sham mouse brains (Figure 3B). There were no remarkable changes in lysophosphatidylcholine isoforms with the

use of autotaxin inhibitors compared with results in the sham group. PF8380 acts as a substrate for competitive and tight-binding inhibition of autotaxin activity.²⁶ In contrast, inhibition of autotaxin by HA130 results from a combination of a decreased turnover number and reduced affinity for its substrate.²⁵ LPA isoforms were then measured in the plasma of sham, I/R, and HA130- and PF8330-treated mice. The elevated levels of LPA isoforms (18:1, 16:0, 18:0, 20:4, and 22:6) observed in I/R mouse brain tissue were significantly blunted by the use of either HA130 or PF8380 (Figure 3C). None of the other isoforms of LPA showed any significant alteration between the groups. These results demonstrate that autotaxin activity and LPA elevation can be managed with the use of autotaxin inhibitors.

Autotaxin Inhibitors and an LPA Receptor Inhibitor Rescue Mitochondrial Bioenergetics Following I/R

Mitochondrial bioenergetics studies reveal the healthy state of cells, providing a snapshot of the status of the tissues. To evaluate the oxidation-reduction status of the brain tissue, we performed OCR analysis in the mitochondria isolated from the brain tissue for all the groups (sham, I/R, HA130, and PF8330). The spare respiratory capacity, ATP turnover, and maximal respiration were significantly decreased in the I/R group compared with those of the sham group. Treatment with HA130 or PF8380 significantly reverted the basal respiration, spare respiratory capacity, ATP turnover, and maximal respiration to near-normal levels compared with results in the I/R group (Figure 3D through 3F). In addition to autotaxin inhibitors, we also used BrP-LPA, which is an autotaxin inhibitor plus LPA pan receptor inhibitor.^{26,27} The autotaxin-LPA-LPA receptor is the classic action pathway for LPA, and as we observed increased LPA receptor expression (LPAR1/LPAR2/LPAR5/LPAR6; Figure 2E), we were interested in using BrP-LPA in our ischemic stroke model. BrP-LPA was able to revert the basal OCR and FCCP OCR, which ultimately led to a significant increase in the spare respiratory capacity, ATP turnover, and maximal respiration in mitochondria when compared with those in the I/R group. These findings suggest

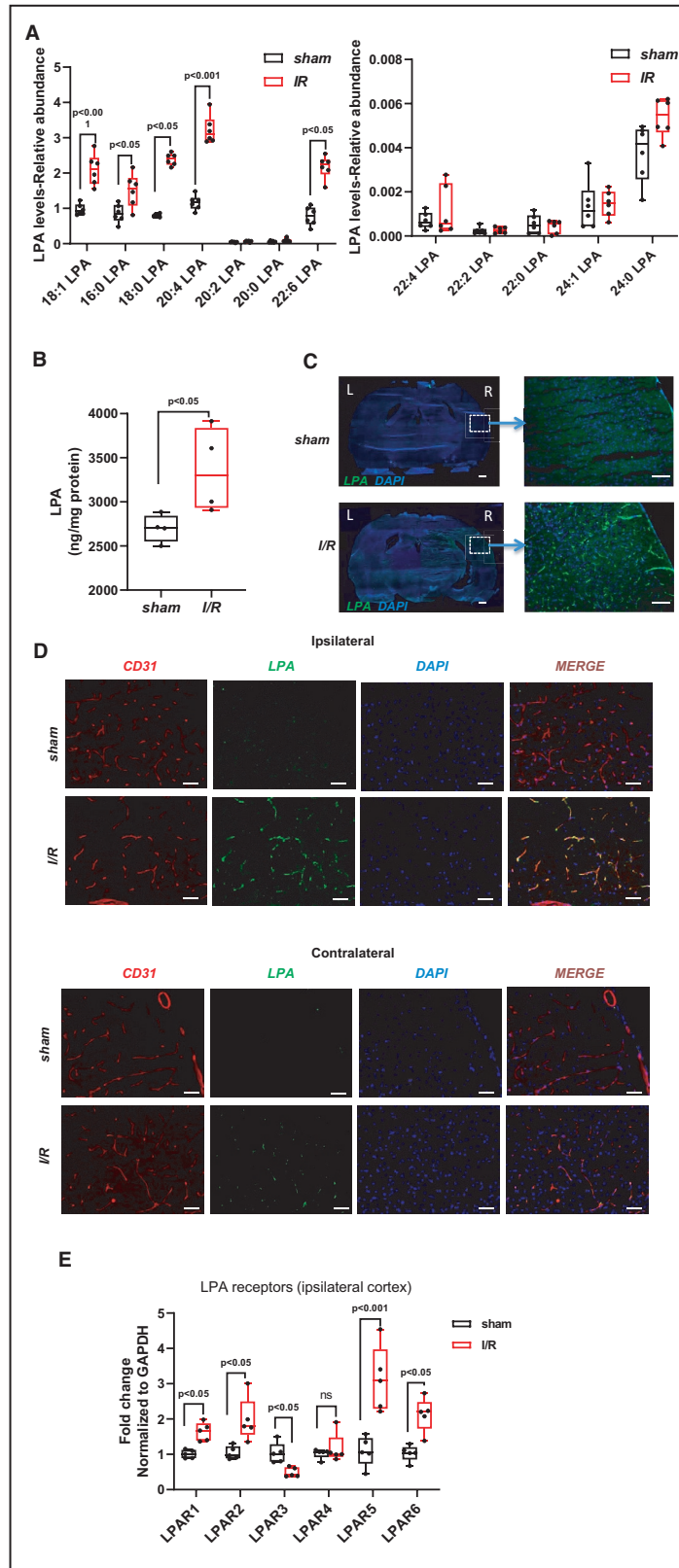
that autotaxin activity or LPA receptor inhibition could be beneficial for maintaining intact mitochondrial function in stroke.

Autotaxin Inhibitors and LPA Receptor Inhibitor Attenuated Antioxidant Status in I/R Mice and Attenuated BBB Dysfunction

As a measure of physiological outcome, TTC staining was performed in mice brain sections. In TTC stainings performed in the treatment groups (HA130/PF8330/BrP-LPA), the infarct region was significantly reduced compared with that of the I/R (Figure 4A), suggesting reduced stroke exacerbation with the use of these inhibitors. Oxidative stress is increased in many diseases, including stroke, which disrupts the oxidative balance of the cells, ultimately altering the antioxidants. Cells are equipped with a range of antioxidants, so we wanted to examine the antioxidant status in our experimental groups. Because superoxide is a crucial indicator of oxidative stress, we measured the superoxide levels in brain tissues. With I/R, there was a >2-fold (Figure 4B) increase in the levels of superoxide in the brain tissue compared with those in the sham brain tissue. All 3 inhibitors (HA130, PF8380, and BrP-LPA) significantly lowered the superoxide levels in brain tissue compared with levels in I/R (Figure 4B). As superoxide dismutase (SOD) is the primary enzyme responsible for quenching superoxide, an SOD activity assay was performed in which the reduction of both MnSOD and CuZnSOD (Figure 4C) was observed in I/R mice compared with that in sham mice. SOD activity for MnSOD and CuZnSOD was rescued on the use of autotaxin inhibitors and an LPA receptor inhibitor (Figure 4C). Catalase and glutathione peroxidase are antioxidant enzymes that also challenge the oxidative stress caused by reactive oxygen species during tissue injury. With I/R, catalase activity and glutathione peroxidase activity declined significantly, whereas HA130, PF8380, or BrP-LPA rescued the enzymatic activities of these antioxidants (Figure 4C and 4D), demonstrating attenuation of LPA-mediated oxidative stress in the brain tissue. In line with the reduced glutathione peroxidase activity, it was expected that we would detect decreased glutathione levels in I/R mice brains

Figure 2. Lysophosphatidic acid (LPA) escalation following ischemia and reperfusion (I/R).

A, LPA subspecies in plasma from sham and I/R mice, measured with high-performance liquid chromatography–tandem mass spectrometry (liquid chromatography–mass spectrometry), quantified relative to 18:1 LPA. **B**, LPA ELISA immunoassay performed in ipsilateral brain tissue lysate and quantified as ng/mg protein in sham and I/R. **C**, Mouse brain cryosections stained for LPA (green fluorescence) and 4',6-diamidino-2-phenylindole (DAPI) (blue fluorescence) in sham and I/R mice; the arrows show magnified images of the respective regions in the brain. Bar=1 mm for the whole brain, and bar=500 μm for magnified images. **D**, Immunofluorescence in mouse brain cryosections performed for LPA and cluster of differentiation 31 (CD31) in sham and I/R on ipsilateral and contralateral cortex. Bar=200 μm. **E**, LPA receptor mRNA expression was measured in brain tissue lysate from sham and I/R mice. All values are mean±SD compared with the sham group using Mann-Whitney *U* test. L indicates left; LPAR, LPA receptor; OCR, oxygen consumption rate; and R, right.



compared with those of sham brains. The glutathione level was significantly revived with the use of HA130, PF8380, or BrP-LPA (Figure 4F) when compared with

I/R. These data show that autotaxin inhibitors and the LPA receptor inhibitor were able to restore a variety of potent antioxidants in I/R.

Figure 3. Autotaxin (ATX) inhibitors in middle cerebral artery occlusion decrease ATX activity and lysophosphatidic acid (LPA).

A, Enzymatic activity test for ATX, measured with AR-2 fluorescence, quantified as relative fluorescence unit (RFU), in sham, ischemia and reperfusion (I/R), HA130, and PF8380 mouse brain slices. **B**, Lysophosphatidylcholine (LPC) subspecies in plasma from sham, I/R, HA130, and PF8380 mice measured with high-performance liquid chromatography–tandem mass spectrometry (liquid chromatography–mass spectrometry [LC-MS]) quantified relative to 18:1 LPC. **C**, LPA subspecies in plasma from sham, I/R, HA130, and PF8380 mice measured with LC-MS, quantified relative to 18:1 LPA. **D** and **E**, Graph represents oxygen consumption rate (OCR) (pmol/min per μ g protein) measurements in isolated mitochondria from sham, I/R, HA130, PF8380, or BrP-LPA mouse brain tissue at baseline and after sequential addition of oligomycin, carbonyl cyanide p-trifluoro-methoxyphenyl hydrazone (FCCP), and antimycin A+rotenone. **F**, Spare respiratory capacity, ATP turnover, and maximum respiration values analyzed in sham, I/R, HA130, PF8380, or BrP-LPA mice. All values are mean \pm SD. * P <0.05, ** P <0.01 (1-way ANOVA, followed by the Tukey, post hoc test, was performed).

Increased BBB permeability after stroke is one of the main problems that exacerbate the disease. We wanted to observe permeability in all of our experimental groups as a measure of the extent of stroke pathology. Evans blue fluorescence analysis was used to determine the level of permeability in mice brains in real time using a Li-COR Odyssey imager. In the brains of mice with the I/R injury, there was an apparent increase in permeability, which was elevated almost 3-fold compared with that in the sham mice. HA130, PF8380, or BrP-LPA injection treatment significantly attenuated the permeability of the BBB (Figure 5A). Further along, the effect of inhibitors was evaluated with immunofluorescence of the junctional proteins in sham, I/R, HA130, PF8380, and BrP-LPA mice brains. Ipsilateral cortex staining of junctional proteins for claudin-5 (Figure 5B), zonula occludens-1 (Figure 5C), VE-cadherin (Figure S1), and β -catenin (Figure S2) was performed. A clear observation of improved modulation of junctional proteins was observed with the use of HA130, PF8380, or BrP-LPA (Figure 5B and 5C) compared with the I/R. So, the maintenance of junctional proteins should decrease the risk of BBB dysfunction and hemorrhage.

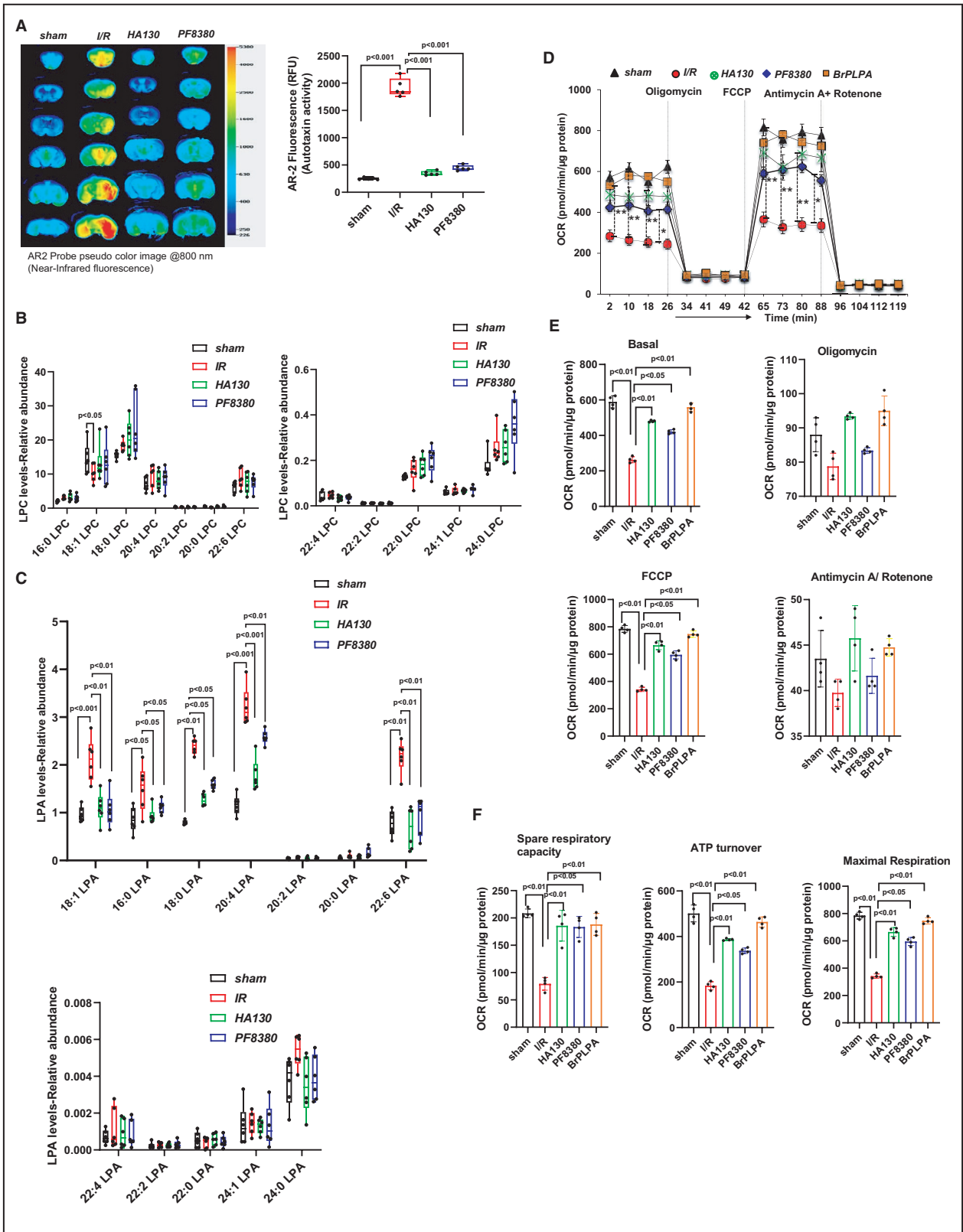
DISCUSSION

Ischemic stroke has only one clinically approved treatment, recombinant tPA, apart from the clinical intervention of mechanical thrombectomy. Unfortunately, this treatment is not inclusive, as <5% of patients can receive treatment² because of hemorrhagic transformation.²⁹ Therefore, studies have begun to focus on developing a more comprehensive therapeutic agent. Studies suggest that a leading cause of stroke exacerbation is BBB disruption following I/R.^{10,30} Preservation of the integrity of the BBB has become an important focus when addressing the therapeutic issues related to ischemic stroke.^{31,32} Molecules and signaling pathways in the brain, particularly in endothelial cells, are targeted for this purpose.^{7–9} In this study, we addressed the role of the autotaxin-LPA axis in a mouse model of transient focal cerebral ischemia. In our stroke model, an ischemic infarct was detected in the right hemisphere of the mouse brain following I/R. We

observed microglial activation in the ipsilateral brain sections following MCAO. Following I/R, levels of the LPA producer autotaxin were increased at the mRNA level in the peri-infarct region, suggesting that reactive oxygen species generation^{33,34} in stroke might stimulate the signal. Autotaxin converts lysophosphatidylcholine to LPA, so we performed an autotaxin activity assay using AR-2 fluorescence in real time, detecting an almost 4-fold higher autotaxin enzymatic activity in the brains of mice subjected to I/R. When plasma lysophosphatidylcholine was analyzed using mass spectrometry, we observed no change in the different species of lysophosphatidylcholine following MCAO, except for a reduction in the 18:1 species. Thus, autotaxin was observed to be upregulated following ischemic stroke.

LPA is essential for basic cellular signaling in healthy cells; however, in diseased conditions, such as atherosclerosis,³⁵ hypertension,³⁶ traumatic brain injury,^{37,38} Alzheimer disease,³⁹ myocardial infarction,^{40,41} pulmonary fibrosis,⁴² and cancer,^{43,44} the elevation of LPA has been observed in local tissue as well as in blood. Therefore, we examined LPA in plasma following I/R using mass spectrometry and in localized tissue using the LPA antibody in brain sections. We observed increased autotaxin activity on the ipsilateral side in mouse brain tissues, resulting in increased plasma and tissue levels of LPA in I/R mice. LPA was elevated in tissue level in the brain following I/R observed by ELISA along with the plasma level. Detection of LPA in localized brain tissue of I/R mouse brain cryosections also displayed an increased accumulation of LPA in the brain tissue, both in and around the ischemic core tissue. In line with our observations, Ueda et al⁴⁵ reported an increase in several species of LPA, mainly in the sensory cortex, with cerebral infarction.

Interestingly, we detected LPA being colocalized with brain microvasculature when LPA and cluster of differentiation 31 were costained in brain cryosections, indicating LPA elevation specifically in brain microvessels with I/R. Our observation suggests that the enhanced microvascular permeability following ischemic stroke is mediated partly through increased LPA signaling in the microvasculature. LPA signals downstream through its receptors, and



with I/R injury, mRNA expression levels of LPAR1, LPAR2, LPAR5, and LPAR6 increased significantly in the peri-infract region. However, LPAR3 mRNA expression levels were reduced considerably, with no

apparent changes observed in LPAR4 expression levels. Previously, we showed that lung endothelial permeability is partly mediated through LPAR4.²⁶ Our current findings further attest that BBB integrity

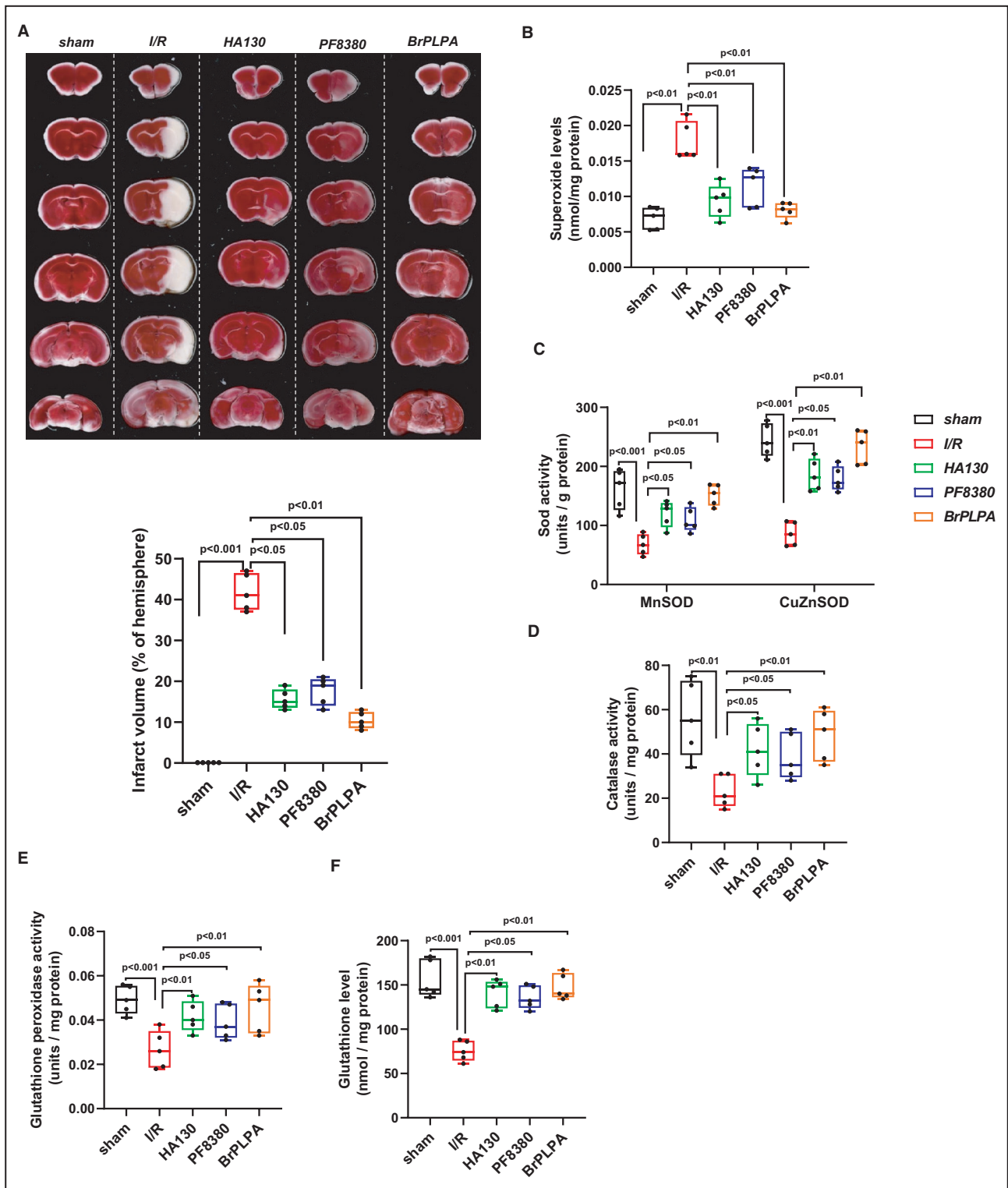


Figure 4. Biochemical assays improved with the use of inhibitors.

A, Triphenyl tetrazolium chloride staining of mouse brain slices and respective infarct volume (percentage of the hemisphere) measured in sham, ischemia and reperfusion (I/R), HA130, PF8380, or BrP-LPA mice (n=5 in each group). **B**, Superoxide measured using high-performance liquid chromatography in brain tissue lysate after staining with a dihydroethidium fluorescence probe in sham, I/R, HA130, PF8380, or BrP-LPA mice. **C** through **E**, Superoxide dismutase (SOD) activity, catalase activity, and glutathione peroxidase activity quantified in brain tissue lysate from sham, I/R, HA130, PF8380, or BrP-LPA mice. **F**, Glutathione levels were measured in sham, I/R, HA130, PF8380, or BrP-LPA mice. All values are mean±SD (1-way ANOVA, followed by the Tukey, post hoc test, was performed).

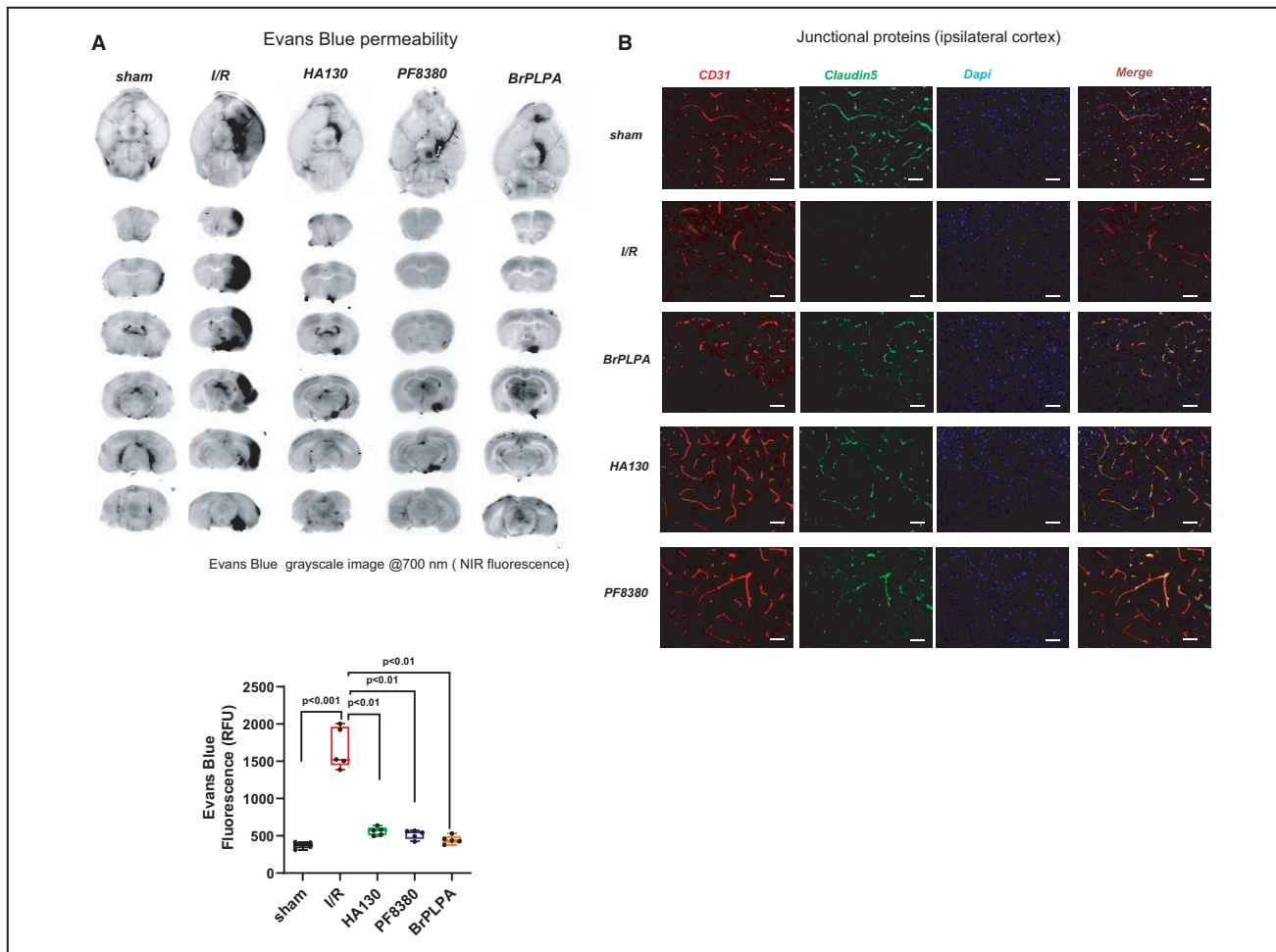


Figure 5. Improved endothelial permeability with the use of inhibitors.

A, Evans blue fluorescence measured and quantified with relative fluorescence unit (RFU) in whole brains of sham, ischemia and reperfusion (I/R), HA130, PF8380, or BrP-LPA mice. **B**, Immunofluorescence staining for claudin-5 in ipsilateral cortex of sham, I/R, HA130, PF8380, or BrP-LPA mice. **C**, Immunofluorescence staining for zonula occludens-1 in ipsilateral cortex of sham, I/R, HA130, PF8380, or BrP-LPA mice. Bar=200 μ m. All values are mean \pm SD (1-way ANOVA, followed by the Tukey, post hoc test, was performed). CD31 indicates cluster of differentiation 31; and DAPI, 4',6'-diamidino-2-phenylindole.

differs from the endothelial barrier integrity observed elsewhere.⁴⁶ LPAR5 has been found to be involved in inflammation through microglial activation,^{47,48} so the several-fold elevation observed following I/R could be from activated microglia. LPAR1 has previously been shown to be involved with cell migration proliferation⁴⁹ and contraction.^{50,51} In our study, we have observed that LPAR1 is the dominant player mediating the permeability in brain microvascular endothelial cells (data not shown).

Autotaxin inhibitors are believed to be beneficial in cancer,⁵² pulmonary fibrosis,⁵³ and other diseases.⁵⁴ The actions of these inhibitors in stroke have not been adequately explored, so we used 2 inhibitors, HA130 and PF8380, in our study of I/R. Following treatment with either of the autotaxin inhibitors, the initial increase in autotaxin activity in I/R was significantly lowered, with HA130 being more effective than PF8380. Liquid

chromatography–mass spectrometry analysis revealed no particular alteration in the lysophosphatidylcholine species after the use of inhibitors compared with results in the sham group, suggesting a potent blockade of autotaxin activity. As lysophosphatidylcholine is the precursor of LPA and autotaxin catalyzes lysophosphatidylcholine, it was apparent that the autotaxin inhibitors caused no specific changes to the lysophosphatidylcholine isoforms. Nevertheless, on treatment with the autotaxin inhibitors, the levels of LPA isoforms 18:1, 16:0, 18:0, 20:4, and 22:6 decreased, when they had been significantly elevated with I/R. Both the autotaxin inhibitors were efficient in lowering the plasma LPA level.

It has been established that following stroke, oxidative stress is induced, and furthermore, that oxidative stress is enhanced with reperfusion.^{55–58} Mitochondria are directly affected by oxidative stress

in various neuronal diseases.⁵⁹ The mitochondria from the mouse brain tissue showed reduced mitochondrial bioenergetics (ie, reduced basal OCR with decreased spare capacity, ATP turnover, and maximal respiration following I/R injury). However, following treatment with HA130, PF8380, or BrP-LPA, the OCR level improved, suggesting that the increased autotaxin/LPA axis in I/R has a negative effect on mitochondrial bioenergetics.

LPA has been shown to cause permeability in various organs, such as the lungs,⁶⁰ via modulation of its receptors. In our I/R model, we used Evans blue dye to measure permeability in real time using a LiCOR Odyssey imager. The inhibitors HA130, PF8380, and BrP-LPA limited permeability, showing that autotaxin/LPA receptor inhibitors reduced damage to the BBB. We also observed that the junctional proteins, such as claudin-5, zonula occludens-1, VE-cadherin, and β -catenin, were improved in inhibitor-treated groups along with the improved Evans blue permeability. It has been previously shown that intact junctional proteins can be considered therapeutic targets for stroke management.^{6,9,61} With further mechanistic study, autotaxin/LPA receptor inhibitors could be included in the ischemic stroke treatment strategy for improved BBB function. In addition to mitochondrial impairment and permeability, we observed a reduction in the cellular antioxidant activity of enzymes, such as catalase, MnSOD, and glutathione peroxidase, signifying oxidation-reduction imbalance with I/R. The oxidation-reduction capacity in I/R mouse brains was restored to near normal on treatment with HA130, PF8380, or BrP-LPA. In addition, the overall superoxide levels in the brain, which were amplified following I/R, were also controlled on treatment with autotaxin/LPA receptor inhibitors. These findings suggest that cellular oxidative stress could be limited, and reactive oxygen species toxicity is counterbalanced by using autotaxin/LPA receptor inhibitors, ultimately rescuing brain tissue following ischemic stroke.

LPA was observed to disrupt mitochondrial function, oxidation-reduction balance, and BBB. The findings in this study suggest that inhibition of LPA or its receptors limits the mitochondrial damage caused by LPA. Mice with a heterozygous autotaxin deficiency were associated with improved mitochondrial energy metabolism when exposed to a high-fat, high-sucrose diet.⁶² Recently, we showed that cells exposed to LPA demonstrated decreased mitochondrial oxidative phosphorylation.¹⁸ In this study, we pursued defining the role of autotaxin and LPA in ischemic stroke, focusing on BBB disruption, as restriction of vascular permeability limits the exacerbation of the disease. With the increase of autotaxin and LPA in brain tissue through I/R, the downstream effects of LPA in endothelial cells

provide more insight into the development of an efficient therapeutic agent. Remedies can be designed at different levels, such as the use of autotaxin inhibitors, LPA receptor inhibitors, or downstream signaling molecules to target permeability. As in our study, recent research by Strumwasser et al⁶³ in rat mesenteric postcapillary venules discusses the probability of controlling permeability following I/R injury by inhibiting autotaxin. Katsifa et al⁶⁴ have shown that autotaxin activity is dispensable for the adult mouse. Because autotaxin seems to be a nonessential enzyme for adults, compared with other approaches, the alteration of this enzyme may be a safer option to pursue in combating disease. With this in mind, better therapeutics for ischemic stroke could be formulated.

ARTICLE INFORMATION

Received June 28, 2021; accepted July 30, 2021.

Affiliations

Department of Cellular Biology and Anatomy (S.B., S.S., H.A., U.S., G.S., C.L., S.M., M.P.), Department of Pathology and Translational Pathobiology (M.S.B., C.K.), School of Medicine (W.P.A., M.T.M.), and Division of Cardiology, Department of Internal Medicine (S.M., M.P.), Louisiana State University Health Sciences Center, Shreveport, LA.

Acknowledgments

The authors thank the Center for Cardiovascular Disease and Sciences imaging and the Animal Care Committee, and the veterinary staff at Louisiana State University Health Sciences Center–Shreveport for their help with animal experiments at the vivarium. The authors thank the Virginia Commonwealth University (VCU) Lipidomics/Metabolomics Core, the National Institutes of Health—National Cancer Institute Cancer Center Support Grant P30 CA016059, the VCU Massey Cancer Center, and the shared resource grant (S10RR031535) from the National Institutes of Health for help in performing the mass spectrometry analysis.

Sources of Funding

This work was supported by Louisiana State University Health Sciences–Shreveport Intramural Grant 110101074A to Dr Miriyala; National Institutes of Health grants HL141998 and HL141998-01S1 to Dr Miriyala; grants AA025744, AA026708, and AA025744-02S1 to Dr Panchatcharam; grants HL122354 and HL145753 to Dr Bhuiyan; and grant P20GM121307 to Dr Kevil. Dr Panchatcharam provided funding to pay the publication charges for this article.

Disclosures

None.

Supplementary Material

Data S1
Figures S1–S2
Reference 65

REFERENCES

1. Rajsic S, Gothe H, Borba HH, Sroczynski G, Vujicic J, Toell T, Siebert U. Economic burden of stroke: a systematic review on post-stroke care. *Eur J Health Econ*. 2019;20:107–134. doi: 10.1007/s10198-018-0984-0
2. Kassner A, Merali Z. Assessment of blood-brain barrier disruption in stroke. *Stroke*. 2015;46:3310–3315. doi: 10.1161/STROKE.EAHA.115.008861
3. Josephson SA, Kamel H. The acute stroke care revolution: enhancing access to therapeutic advances. *JAMA*. 2018;320:1239–1240. doi: 10.1001/jama.2018.11122

4. Cohen DL, Kearney R, Griffiths M, Nadesalingam V, Bathula R. Around 9% of patients with ischaemic stroke are suitable for thrombectomy. *BMJ*. 2015;351:h4607. doi: 10.1136/bmj.h4607
5. Chia NH, Leyden JM, Newbury J, Jannes J, Kleinig TJ. Determining the number of ischemic strokes potentially eligible for endovascular thrombectomy: a population-based study. *Stroke*. 2016;47:1377–1380. doi: 10.1161/STROKEAHA.116.013165
6. Sandoval KE, Witt KA. Blood-brain barrier tight junction permeability and ischemic stroke. *Neurobiol Dis*. 2008;32:200–219. doi: 10.1016/j.nbd.2008.08.005
7. Sifat AE, Vaidya B, Abbruscato TJ. Blood-brain barrier protection as a therapeutic strategy for acute ischemic stroke. *AAPS J*. 2017;19:957–972. doi: 10.1208/s12248-017-0091-7
8. Merali Z, Huang K, Mikulis D, Silver F, Kassner A. Evolution of blood-brain-barrier permeability after acute ischemic stroke. *PLoS One*. 2017;12:e0171558. doi: 10.1371/journal.pone.0171558
9. Abdullahi W, Tripathi D, Ronaldson PT. Blood-brain barrier dysfunction in ischemic stroke: targeting tight junctions and transporters for vascular protection. *Am J Physiol Cell Physiol*. 2018;315:C343–C356. doi: 10.1152/ajpcell.00095.2018
10. Jiang X, Andjelkovic AV, Zhu L, Yang T, Bennett MVL, Chen J, Keep RF, Shi Y. Blood-brain barrier dysfunction and recovery after ischemic stroke. *Prog Neurobiol*. 2018;163–164:144–171. doi: 10.1016/j.pneurobio.2017.10.001
11. Pages C, Simon MF, Valet P, Saulnier-Blache JS. Lysophosphatidic acid synthesis and release. *Prostaglandins Other Lipid Mediat*. 2001;64:1–10. doi: 10.1016/S0090-6980(01)00110-1
12. Salous AK, Panchatcharam M, Sunkara M, Mueller P, Dong A, Wang Y, Graf GA, Smyth SS, Morris AJ. Mechanism of rapid elimination of lysophosphatidic acid and related lipids from the circulation of mice. *J Lipid Res*. 2013;54:2775–2784. doi: 10.1194/jlr.M039685
13. Ishii I, Fukushima N, Ye X, Chun J. Lysophospholipid receptors: signaling and biology. *Annu Rev Biochem*. 2004;73:321–354. doi: 10.1146/annurev.biochem.73.011303.073731
14. Yun C, Yung NCS, Chun J. LPA receptor signaling: pharmacology, physiology, and pathophysiology. *J Lipid Res*. 2014;55:1192–1214. doi: 10.1194/jlr.R046458
15. Lin ME, Herr DR, Chun J. Lysophosphatidic acid (LPA) receptors: signaling properties and disease relevance. *Prostaglandins Other Lipid Mediat*. 2010;91:130–138. doi: 10.1016/j.prostaglandins.2009.02.002
16. Tsukahara T, Matsuda Y, Hanui H. Lysophospholipid-related diseases and PPARgamma signaling pathway. *Int J Mol Sci*. 2017;18:2730.
17. Kou R, Igarashi J, Michel T. Lysophosphatidic acid and receptor-mediated activation of endothelial nitric-oxide synthase. *Biochemistry*. 2002;41:4982–4988. doi: 10.1021/bi016017r
18. Chandra M, Escalante-Alcalde D, Bhuiyan MS, Orr AW, Kevil C, Morris AJ, Nam H, Dominic P, McCarthy KJ, Miriyala S, et al. Cardiac-specific inactivation of LPP3 in mice leads to myocardial dysfunction and heart failure. *Redox Biol*. 2018;14:261–271. doi: 10.1016/j.redox.2017.09.015
19. Vazquez-Medina JP, Dodia C, Weng L, Mesaros C, Blair IA, Feinstein SI, Chatterjee S, Fisher AB. The phospholipase A2 activity of peroxiredoxin 6 modulates NADPH oxidase 2 activation via lysophosphatidic acid receptor signaling in the pulmonary endothelium and alveolar macrophages. *FASEB J*. 2016;30:2885–2898.
20. Chen C, Ochoa LN, Kagan A, Chai H, Liang Z, Lin PH, Yao Q. Lysophosphatidic acid causes endothelial dysfunction in porcine coronary arteries and human coronary artery endothelial cells. *Atherosclerosis*. 2012;222:74–83. doi: 10.1016/j.atherosclerosis.2012.02.010
21. Sarker MH, Hu DE, Fraser PA. Regulation of cerebrovascular permeability by lysophosphatidic acid. *Microcirculation*. 2010;17:39–46. doi: 10.1111/j.1549-8719.2010.00001.x
22. Schulze C, Smales C, Rubin LL, Staddon JM. Lysophosphatidic acid increases tight junction permeability in cultured brain endothelial cells. *J Neurochem*. 1997;68:991–1000. doi: 10.1046/j.1471-4159.1997.68030991.x
23. On NH, Savant S, Toews M, Miller DW. Rapid and reversible enhancement of blood-brain barrier permeability using lysophosphatidic acid. *J Cereb Blood Flow Metab*. 2013;33:1944–1954. doi: 10.1038/jcbfm.2013.154
24. Madan D, Ferguson CG, Lee WY, Prestwich GD, Testa CA. Non-invasive imaging of tumors by monitoring autotaxin activity using an enzyme-activated near-infrared fluorogenic substrate. *PLoS One*. 2013;8:e79065. doi: 10.1371/journal.pone.0079065
25. Albers HMG, Dong A, van Meeteren LA, Egan DA, Sunkara M, van Tilburg EW, Schuurman K, van Tellingen O, Morris AJ, Smyth SS, et al. Boronic acid-based inhibitor of autotaxin reveals rapid turnover of LPA in the circulation. *Proc Natl Acad Sci USA*. 2010;107:7257–7262. doi: 10.1073/pnas.1001529107
26. Panchatcharam M, Salous AK, Brandon J, Miriyala S, Wheeler J, Patil P, Sunkara M, Morris AJ, Escalante-Alcalde D, Smyth SS. Mice with targeted inactivation of ppap2b in endothelial and hematopoietic cells display enhanced vascular inflammation and permeability. *Arterioscler Thromb Vasc Biol*. 2014;34:837–845. DOI: 10.1161/ATVBAHA.113.302335
27. Zhang H, Xu X, Gajewiak J, Tsukahara R, Fujiwara Y, Liu J, Fells JI, Perygin D, Parrill AL, Tigyi G, et al. Dual activity lysophosphatidic acid receptor pan-antagonist/autotaxin inhibitor reduces breast cancer cell migration in vitro and causes tumor regression in vivo. *Cancer Res*. 2009;69:5441–5449. DOI: 10.1158/0008-5472.CAN-09-0302
28. Ryu HW, Lim W, Jo D, Kim S, Park JT, Min JJ, Hyun H, Kim HS. Low-dose Evans blue dye for near-infrared fluorescence imaging in photothrombotic stroke model. *Int J Med Sci*. 2018;15:696–702. doi: 10.7150/ijms.24257
29. Wang W, Li M, Chen Q, Wang J. Hemorrhagic transformation after tissue plasminogen activator reperfusion therapy for ischemic stroke: mechanisms, models, and biomarkers. *Mol Neurobiol*. 2015;52:1572–1579. doi: 10.1007/s12035-014-8952-x
30. Hoffmann A, Dege T, Kunze R, Ernst A-S, Lorenz H, Böhler L-I, Korff T, Marti HH, Heiland S, Bendszus M, et al. Early blood-brain barrier disruption in ischemic stroke initiates multifocally around capillaries/venules. *Stroke*. 2018;49:1479–1487. doi: 10.1161/STROKEAHA.118.020927
31. Zhang W, Zhu L, An C, Wang R, Yang L, Yu W, Li P, Gao Y. The blood brain barrier in cerebral ischemic injury—disruption and repair. *Brain Hemorrhages*. 2020;1:34–53. doi: 10.1016/j.hest.2019.12.004
32. Li Y, Zhong W, Jiang Z, Tang X. New progress in the approaches for blood-brain barrier protection in acute ischemic stroke. *Brain Res Bull*. 2019;144:46–57. doi: 10.1016/j.brainresbull.2018.11.006
33. Rodrigo R, Fernandez-Gajardo R, Gutierrez R, Matamala JM, Carrasco R, Miranda-Merchak A, Feuerhake W. Oxidative stress and pathophysiology of ischemic stroke: novel therapeutic opportunities. *CNS Neurol Disord Drug Targets*. 2013;12:698–714.
34. Duris K, Rolland WB, Zhang JH. Stroke pathophysiology and reactive oxygen species. In: Laher I, ed. *Systems Biology of Free Radicals and Antioxidants*. Springer Berlin Heidelberg; 2014:1979–1997.
35. Cui MZ. Lysophosphatidic acid effects on atherosclerosis and thrombosis. *Clin Lipidol*. 2011;6:413–426. doi: 10.2217/clp.11.38
36. Xu YJ, Aziz OA, Bhugra P, Arneja AS, Mendis MR, Dhalla NS. Potential role of lysophosphatidic acid in hypertension and atherosclerosis. *Can J Cardiol*. 2003;19:1525–1536.
37. Crack PJ, Zhang M, Morganti-Kossmann M, Morris AJ, Wojciak JM, Fleming JK, Karve I, Wright D, Sashindranath M, Goldshmit Y, et al. Anti-lysophosphatidic acid antibodies improve traumatic brain injury outcomes. *J Neuroinflammation*. 2014;11:37. doi: 10.1186/1742-2094-11-37
38. Frugier T, Crombie D, Conquest A, Tjhong F, Taylor C, Kulkarni T, McLean C, Pebay A. Modulation of LPA receptor expression in the human brain following neurotrauma. *Cell Mol Neurobiol*. 2011;31:569–577. doi: 10.1007/s10571-011-9650-0
39. Sayas CL, Moreno-Flores MT, Avila J, Wandosell F. The neurite retraction induced by lysophosphatidic acid increases Alzheimer's disease-like Tau phosphorylation. *J Biol Chem*. 1999;274:37046–37052. doi: 10.1074/jbc.274.52.37046
40. Chen X, Yang XY, Wang ND, Ding C, Yang YJ, You ZJ, Su Q, Chen JH. Serum lysophosphatidic acid concentrations measured by dot immunogold filtration assay in patients with acute myocardial infarction. *Scand J Clin Lab Invest*. 2003;63:497–503. doi: 10.1080/00365510310003265
41. Chen J, Chen Y, Zhu W, Han Y, Han B, Xu R, Deng L, Cai Y, Cong X, Yang Y, et al. Specific LPA receptor subtype mediation of LPA-induced hypertrophy of cardiac myocytes and involvement of Akt and NF-kappaB signal pathways. *J Cell Biochem*. 2008;103:1718–1731. DOI: 10.1002/jcb.21564
42. Ninou I, Kaffe E, Muller S, Budd DC, Stevenson CS, Ullmer C, Aidinis V. Pharmacologic targeting of the ATX/LPA axis attenuates bleomycin-induced pulmonary fibrosis. *Pulm Pharmacol Ther*. 2018;52:32–40. doi: 10.1016/j.pupt.2018.08.003
43. Rogers LC, Davis RR, Said N, Hollis T, Daniel LW. Blocking LPA-dependent signaling increases ovarian cancer cell death in response to chemotherapy. *Redox Biol*. 2018;15:380–386. doi: 10.1016/j.redox.2018.01.002

44. Gotoh M, Fujiwara Y, Yue J, Liu J, Lee S, Fells J, Uchiyama A, Murakami-Murofushi K, Kennel S, Wall J, et al. Controlling cancer through the autotaxin-lysophosphatidic acid receptor axis. *Biochem Soc Trans.* 2012;40:31–36. doi: 10.1042/BST20110608
45. Ueda H, Neyama H, Sasaki K, Miyama C, Iwamoto R. Lysophosphatidic acid LPA1 and LPA3 receptors play roles in the maintenance of late tissue plasminogen activator-induced central poststroke pain in mice. *Neurobiol Pain.* 2019;5:100020. doi: 10.1016/j.jnypai.2018.07.001
46. Komarova YA, Kruse K, Mehta D, Malik AB. Protein interactions at endothelial junctions and signaling mechanisms regulating endothelial permeability. *Circ Res.* 2017;120:179–206. doi: 10.1161/CIRCRESAHA.116.306534
47. Plastira I, Joshi L, Bernhart E, Schoene J, Specker E, Nazare M, Sattler W. Small-molecule lysophosphatidic acid receptor 5 (LPAR5) antagonists: versatile pharmacological tools to regulate inflammatory signaling in BV-2 microglia cells. *Front Cell Neurosci.* 2019;13:531. doi: 10.3389/fncel.2019.00531
48. Plastira I, Bernhart E, Goeritzer M, DeVaney T, Reicher H, Hammer A, Lohberger B, Wintersperger A, Zucol B, Graier WF, et al. Lysophosphatidic acid via LPA-receptor 5/protein kinase D-dependent pathways induces a motile and pro-inflammatory microglial phenotype. *J Neuroinflammation.* 2017;14:253. doi: 10.1186/s12974-017-1024-1
49. Sakai N, Chun J, Duffield JS, Wada T, Luster AD, Tager AM. LPA1-induced cytoskeleton reorganization drives fibrosis through CTGF-dependent fibroblast proliferation. *FASEB J.* 2013;27:1830–1846.
50. Van Leeuwen FN, Olivo C, Grivell S, Giepmans BN, Collard JG, Moolenaar WH. Rac activation by lysophosphatidic acid LPA1 receptors through the guanine nucleotide exchange factor Tiam1. *J Biol Chem.* 2003;278:400–406. doi: 10.1074/jbc.M210151200
51. Dancs PT, Ruisanchez É, Balogh A, Panta CR, Miklós Z, Nüsing RM, Aoki J, Chun J, Offermanns S, Tigyi G, et al. LPA(1) receptor-mediated thromboxane A(2) release is responsible for lysophosphatidic acid-induced vascular smooth muscle contraction. *FASEB J.* 2017;31:1547–1555.
52. Valdés-Rives SA, González-Arenas A. Autotaxin-lysophosphatidic acid: from inflammation to cancer development. *Mediators Inflamm.* 2017;2017:9173090. doi: 10.1155/2017/9173090
53. Desroy N, Housseman C, Bock X, Joncour A, Bienvenu N, Cherel L, Labeguere V, Rondet E, Peixoto C, Grassot J-M, et al. Discovery of 2-[[[2-ethyl-6-[4-[2-(3-hydroxyazetidino-1-yl)-2-oxoethyl]piperazin-1-yl]-8-methylimidazo[1,2-a]pyridin-3-yl]methylamino]-4-(4-fluorophenyl)thiazole-5-carbonitrile (GLPG1690), a first-in-class autotaxin inhibitor undergoing clinical evaluation for the treatment of idiopathic pulmonary fibrosis. *J Med Chem.* 2017;60:3580–3590.
54. Zhao Y, Hasse S, Zhao C, Bourgoin SG. Targeting the autotaxin–lysophosphatidic acid receptor axis in cardiovascular diseases. *Biochem Pharmacol.* 2019;164:74–81. doi: 10.1016/j.bcp.2019.03.035
55. Allen CL, Bayraktutan U. Oxidative stress and its role in the pathogenesis of ischaemic stroke. *Int J Stroke.* 2009;4:461–470. doi: 10.1111/j.1747-4949.2009.00387.x
56. Ozkul A, Akyol A, Yenisey C, Arpacı E, Kiyiluglu N, Tataroglu C. Oxidative stress in acute ischemic stroke. *J Clin Neurosci.* 2007;14:1062–1066. doi: 10.1016/j.jocn.2006.11.008
57. Domínguez C, Delgado P, Vilches A, Martín-Gallán P, Ribó M, Santamarina E, Molina C, Corbeto N, Rodríguez-Sureda V, Rosell A, et al. Oxidative stress after thrombolysis-induced reperfusion in human stroke. *Stroke.* 2010;41:653–660. doi: 10.1161/STROKEAHA.109.571935
58. Lakhan SE, Kirchgessner A, Hofer M. Inflammatory mechanisms in ischemic stroke: therapeutic approaches. *J Transl Med.* 2009;7:97. doi: 10.1186/1479-5876-7-97
59. Islam MT. Oxidative stress and mitochondrial dysfunction-linked neurodegenerative disorders. *Neural Res.* 2017;39:73–82. doi: 10.1080/01616412.2016.1251711
60. Ren Y, Guo L, Tang X, Apparsundaram S, Kitson C, Deguzman J, Fuentes ME, Coyle L, Majmudar R, Allard J, et al. Comparing the differential effects of LPA on the barrier function of human pulmonary endothelial cells. *Microvasc Res.* 2013;85:59–67. doi: 10.1016/j.mvr.2012.10.004
61. Lv J, Hu W, Yang Z, Li T, Jiang S, Ma Z, Chen F, Yang Y. Focusing on claudin-5: a promising candidate in the regulation of BBB to treat ischemic stroke. *Prog Neurobiol.* 2018;161:79–96. doi: 10.1016/j.pneurobio.2017.12.001
62. D'Souza K, Nzirorera C, Cowie AM, Varghese GP, Trivedi P, Eichmann TO, Biswas D, Touaibia M, Morris AJ, Aidinis V, et al. Autotaxin-LPA signaling contributes to obesity-induced insulin resistance in muscle and impairs mitochondrial metabolism. *J Lipid Res.* 2018;59:1805–1817. doi: 10.1194/jlr.M082008
63. Strumwasser A, Cohan CM, Beattie G, Chong V, Victorino GP. Autotaxin inhibition attenuates endothelial permeability after ischemia-reperfusion injury. *Clin Hemorheol Microcirc.* 2020;75:399–407. doi: 10.3233/CH-190732
64. Katsifa A, Kaffe E, Nikolaidou-Katsaridou N, Economides AN, Newbigging S, McKerlie C, Aidinis V. The bulk of autotaxin activity is dispensable for adult mouse life. *PLoS One.* 2015;10:e0143083. doi: 10.1371/journal.pone.0143083
65. Spitz DR, Oberley LW. An assay for superoxide dismutase activity in mammalian tissue homogenates. *Anal Biochem.* 1989;179:8–18. doi: 10.1016/0003-2697(89)90192-9

SUPPLEMENTAL MATERIAL

Data S1.

Supplemental Methods

mRNA expression of LPA receptors

Cortical tissues isolated from the peri-infarct area in the ischemia group and the corresponding area in the sham group were used for RNA extraction. Total RNA was extracted from cortical tissues using the Purelink RNA mini kit (Invitrogen) following the manufacturer's instructions. cDNA was prepared with Multiscribe reverse transcriptase enzyme (4368814 High-Capacity cDNA Archive Kit; Applied Biosystems, Foster City, CA), and mRNA expression was measured in a RT-PCR reaction using TaqMan[®] gene expression assays and TaqMan[®] Universal PCR Master Mix (4444556 Applied Biosystems, Foster City, CA) on a Vii7 Real-Time PCR System (Applied Biosystems, Foster City, CA). Receptor expression analysis was done using the Δct method normalized to glyceraldehyde-3-phosphate dehydrogenase (GAPDH). The fold change in expression was calculated using the $2^{-\Delta\Delta\text{CT}}$ method normalized to GAPDH as an endogenous control. Primers used were Mm01346925_m1 (LPA1), Mm00469562_m1 (LPA2), Mm00469694_m1 (LPA3), Mm02620784_s1 (LPA4), Mm02621109_s1 (LPA5), Mm00613058_s1 (LPA6), Mm00516572_m1 (ATX), and Mm99999915_g1 (GAPDH) from Applied Biosystems.

Immunohistochemistry

Mice were euthanized with 100% isoflurane and perfused with 4% paraformaldehyde. Mouse brains were collected and preserved in OCT and then cryosectioned. The brain sections were blocked with 10% goat serum for an hour then permeabilized with 0.2% Triton X-100. The primary antibodies LPA (Z-P200, Echelon Biosciences Inc.) and Iba1 (019-19741, Wako Chemicals) were added overnight at 4 °C. Secondary antibodies were added for 1 hour at room temperature, and the mounted slides were visualized using a fluorescence microscope with a mounted Nikon camera. LPA in tissue lysate was measured using the LPA ELISA kit (LS-F25111-1, LSBio).

Superoxide measurement

A high-performance liquid chromatography (HPLC) system coupled with UV-vis and fluorescence detectors were used for the measurement of superoxide in brain tissue and in MBMEC. For mouse brain tissue, 0.3 mg DHE (DHE-5-ethyl-5, 6-dihydro-6-phenyl-3, 8-diaminophenanthridine; Fluka, 37291) was prepared in DMSO and administered i.p. 1 h before the completion of reperfusion time. Brain tissues were collected after reperfusion and homogenized in 50 mM phosphate buffer (pH 7.4). The supernatant was separated and 100 μL transferred to a tube with 100 μL MeOH/HClO₄ solution. Protein was precipitated by incubating the tube on ice for 2 h. The supernatant was obtained by centrifugation of the tubes at 12,000 $\times g$, 4 °C for 10 min. An aliquot of 100 μL supernatant was added to 100 μL 1 M phosphate buffer (pH 2.6). Excess buffer was removed following centrifugation at 12,000 $\times g$, 4 °C for 5 min. The supernatant was transferred to a new tube to be used for HPLC superoxide measurement.

Biochemical assays

For SOD2 activity, we used the Nitro Blue Tetrazolium (NBT)-bathocuproine sulfonate (Sigma) reduction inhibition method of Spitz and Oberley⁷⁰. Homogenized mouse brain tissues in 50 mM potassium phosphate buffer (pH 7.8) were used for the assay. Sodium cyanide (5 mM; Sigma) was used to inhibit Cu/ZnSOD, allowing measurement of MnSOD activity (units per mg protein). The catalase and glutathione assays were performed in homogenized brain tissues according to the manufacturer's instructions (Catalase Assay Kit, CAT100, and Glutathione Peroxidase Cellular Activity Assay Kit, CGP1, both from Sigma).

Immunofluorescence staining of junctional proteins

For immunofluorescence staining, mice brain cryosections were blocked with 10% goat serum for 1 h, then incubated overnight at 4 °C with mouse anti-ZO-1 (ThermoFisher), mouse anti-claudin-5 (Invitrogen), rabbit anti-VE-cadherin (Santacruz biotechnology), rabbit anti- β -catenin (Santacruz biotechnology) and CD31 (BD biosciences) as primary antibodies. The following secondary antibodies: AlexaFluor 488 goat anti-mouse (ThermoFisher), AlexaFluor 488 goat anti-rabbit (ThermoFisher), or AlexaFluor 594 goat anti-rat (ThermoFisher) were used for 1 h at room temperature. The sections were mounted with Vecta shield mounting medium with DAPI (H-1800, Vector Laboratories) and visualized using a fluorescence microscope with a mounted Nikon camera.

Figure S1. Immunofluorescence staining of Junctional proteins in mice brain.
Immunofluorescence staining for VE-cadherin in ipsilateral brains of sham, I/R, HA130, PF8380, or BrP-LPA mice.

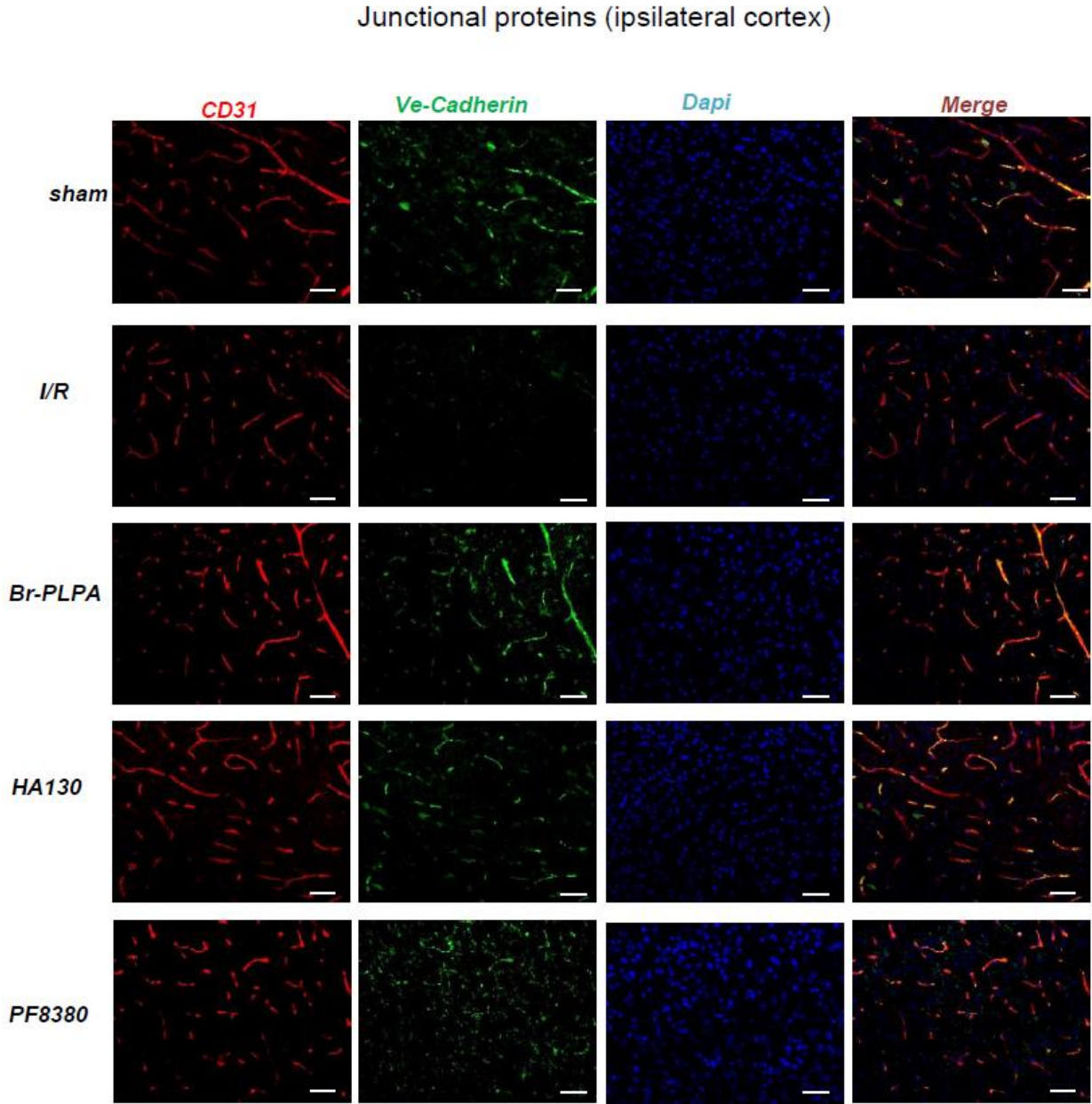


Figure S2. Immunofluorescence staining for β -catenin in ipsilateral brains of sham, I/R, HA130, PF8380, or BrP-LPA mice. Scale bar=200 μ m.

